Deep-Sea Research, Vol. 39, No. 2, pp. 199–219, 1992.
Printed in Great Britain.

0198–0149/92 $5.00 + 0.00
Pergamon Press plc

Physical and biological effects of Los Niños in the eastern tropical Pacific, 1986–1989

PAUL C. FIEDLER,* FRANCISCO P. CHAVEZ,† DAVID W. BEHRINGER‡ and STEPHEN B. REILLY*

(*Received* 30 *May* 1990; *in revised form* 12 *April* 1991; *accepted* 2 *May* 1991)

Abstract—The eastern tropical Pacific Ocean was surveyed in August–November 1986, 1987, 1988 and 1989 as part of a long-term program to monitor dolphin stocks. Temperature, salinity, chlorophyll and nutrients were monitored to help interpret variability in dolphin stock estimates. The four surveys reveal major environmental changes during the moderate 1987 El Niño and the cold La Niña episode that followed in 1988. During the "onset" phase of El Niño in fall 1986, surface temperatures were up to 1.5°C above normal in equatorial water, but near normal in tropical water north of the equator. The equatorial thermocline ridge was deepened by 10–30 m. During the "mature" phase of El Niño in fall 1987, surface temperatures anomalies were up to +2.5°C in equatorial water and about +1°C in tropical water. Thermocline topography was anomalously flat. Surface chlorophyll and nutrient concentrations declined by 11–48% compared to 1986, with the greatest declines occurring in coastal and equatorial upwelling systems and along the countercurrent thermocline ridge. During La Niña 1988, equatorial surface temperatures were up to 2.5°C below normal and the equatorial thermocline ridge was 10–50 m more shallow than normal. Chlorophyll and nitrate concentrations increased by 58–65% compared to 1987. In 1989, surface temperature was within ±1°C of normal throughout the study area and chlorophyll concentrations were similar to those observed in 1986. Changes in nutrient availability and biological productivity during the El Niño/La Niña cycle were caused by variations in both the rate of wind-driven upwelling and in the nutrient content of subsurface water entrained by upwelling.

INTRODUCTION

THE eastern tropical Pacific Ocean (ETP) contains some of the most productive waters of the world oceans (CHAVEZ and BARBER, 1987) and supports important clupeoid and tuna fisheries. Yet, this region has been surveyed on a large scale only during EASTROPAC in 1967–1968 (BLACKBURN *et al.*, 1970). The ETP is also a region of significant interannual variability associated with the El Niño–Southern Oscillation (ENSO), an internally-driven cycle within the coupled ocean–atmosphere system of the tropical Pacific (ENFIELD, 1989). Since ENSO variability has global atmospheric, oceanic and biological ramifications,

*NOAA/NMFS/Southwest Fisheries Science Center, P. O. Box 271, La Jolla, CA 92038, U.S.A.
†Monterey Bay Aquarium Research Institute, 160 Central Ave., Pacific Grove, CA 93950, U.S.A.
‡NOAA/ERL/Atlantic Oceanographic and Meteorological Laboratory, 4301 Rickenbacker Causeway, Miami, FL 33143, U.S.A. Present address: NOAA/NWS/NMC/Climate Analysis Center, 5200 Auth Road, Washington, DC 20233, U.S.A.

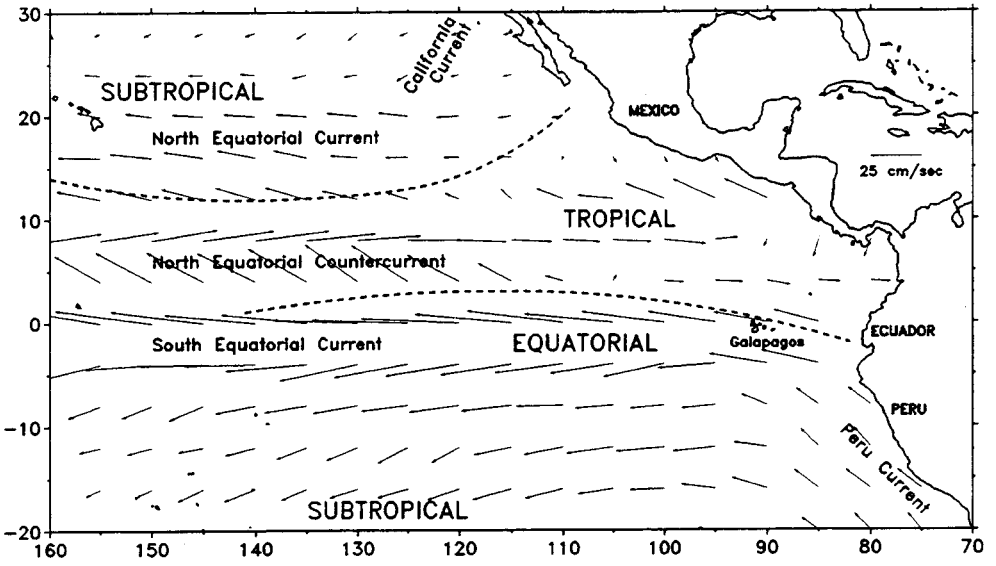

Fig. 1. Eastern tropical Pacific surface water masses (WYRTKI, 1967, 1968) and surface currents (from September–November ship drift data, FIEDLER, in press).

systematic studies of this region are important in order to develop a predictive understanding of the variability. NOAA- and NSF-sponsored studies of the ETP in the last decade (EPOCS, TOGA, TROPIC HEAT) have been restricted to meteorological and physical oceanographic variables (HAYES *et al.*, 1986), with some minor exceptions (e.g. CHAVEZ and BARBER, 1987).

The ETP is the site of a yellowfin tuna purse seine fishery that interacts with large dolphin populations (PERRIN, 1969). In 1986, the National Marine Fisheries Service, Southwest Fisheries Science Center, began a 5-year survey program to monitor trends in dolphin stock abundance in the ETP. Physical and biological data have been collected during dolphin census operations to help interpret variations in stock estimates and to investigate basic questions about dolphin distribution and ecology. We report here the chlorophyll, nutrient and temperature results from the first 4 years of this monitoring program. We discuss spatial patterns of the biological variables, which have never before been measured on this scale in the ETP, and interannual variability associated with El Niño 1986–1987 and La Niña 1988.

BACKGROUND

There are three principal surface water masses in the ETP: tropical surface water, subtropical surface water, and equatorial surface water (Fig. 1). Each of these water masses has characteristic properties determined by climate regimes at local or remote points of origin. Tropical surface water is found in the center of the ETP, along 10°N. It is the warmest, lowest-salinity, and least seasonally variable water in the ETP. Salinity is low

because rainfall exceeds evaporation beneath the cloudy and rainy Intertropical Convergence Zone (ITCZ). Tropical surface water is warmest in May–August, although seasonal variation of temperature is low (≤1°C, HOREL, 1982; FIEDLER, in press). This suggests that seasonal temperature changes are caused by variations in local heating.

Cool, high-salinity subtropical surface water is found toward the poleward edges of the ETP, in the subtropical gyres of the North and South Pacific. In these regions, seasonal variability is higher than in the tropics: SSTs are generally warmest during the summer seasons of the respective hemispheres (HOREL, 1982; FIEDLER, 1991). Evaporation greatly exceeds rainfall, and surface salinity is over 36 psu in the center of the subtropical gyres.

Equatorial surface water is found between the tropical and southern subtropical surface water masses. It appears as the tongue of cool, moderately saline water extending westward along the equator from the Peruvian coast (Fig. 2). In general, equatorial surface water is coldest during northern summer or autumn, when the southeast trade winds are strongest. Seasonal temperature variations are larger near the coast, and the phase of the variations propagates westward from the coast (HOREL, 1982). Thus, the coldest SSTs relative to the annual mean occur in August–September near the coast while at 140°W, for example, the coldest SSTs occur in November.

Conflicting theories suggest that the average state of the cold tongue is maintained either by equatorial upwelling and advection of cold water from the Peru Current by the South Equatorial Current (WYRTKI, 1981) or by the eastward advection of cold water by the Equatorial Undercurrent as it rises to the surface near 95°W (BRYDEN and BRADY, 1985). Whichever mechanism may be correct for the average state, advection of water by the SEC may play an important role in variations of sea surface temperature in the cold tongue (cf. LEETMAA, 1983).

In addition to the three oceanic surface water masses, the cool, low-salinity waters of the Peru and California Currents are also found in the ETP. Peru Current water is contiguous with equatorial surface water. Along the Central American coast, small and ephemeral water masses containing cool, recently upwelled water may be present.

The general features of the surface current system (Fig. 1) can be deduced from the average thermocline topography (Fig. 2). The 20°C isotherm is found in the middle of the thermocline and its depth is used to represent thermocline depth in the tropical Pacific (DONGUY and MEYERS, 1987). The depth of the thermocline indicates the thickness of the surface mixed layer within which wind-driven surface currents flow. The westward transport of surface water by the trade winds results in a downward slope of the thermocline, and upward slope of the sea surface, across the tropical Pacific from east to west. Thermocline topography also has a series of zonal ridges and troughs. We use the traditional names of ridges and troughs in sea-level or dynamic height (WYRTKI, 1974) to label the corresponding subsurface troughs and ridges in the thermocline topography.

In accordance with simple geostrophic theory, the spatial variations of the depth of the thermocline reflect the directional tendencies of the largely zonal, near-surface currents of the ETP. In the northern hemisphere the thermocline will be deeper to the right of a current as the observer looks downstream, while in the southern hemisphere the opposite is true. Thus, the broadest current in the ETP, the South Equatorial Current (SEC), flows westward through the region, extending in the cross-stream direction from the southern edge of the ETP across the equator to almost 5°N. North of the countercurrent thermocline ridge at 10°N, where the thermocline slopes downward to the north, the North Equatorial Current (NEC) also flows westward. Along the eastern boundary, the

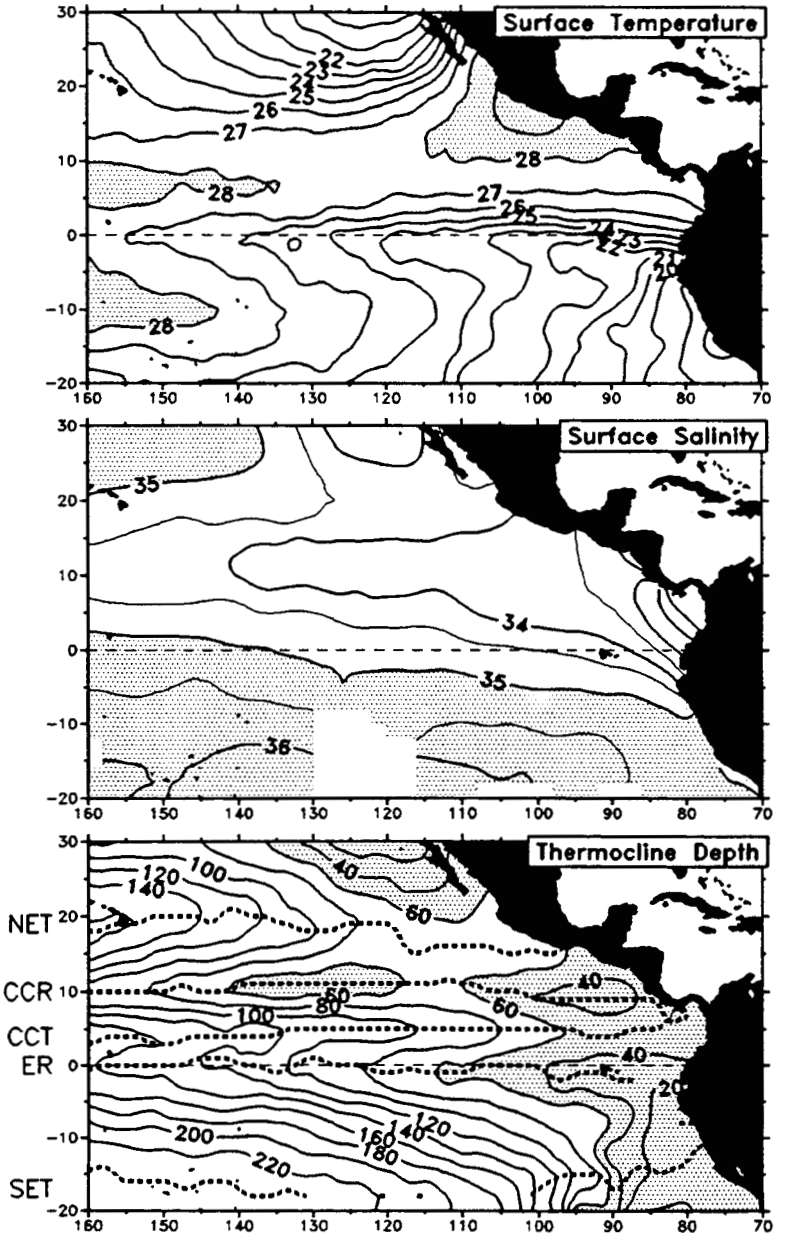

Fig. 2. August–November climatological fields (FIEDLER, in press). (Top) Surface temperature (°C), 1928–1988, n = 70,700. (Middle) Surface salinity (psu), 1922–1988, n = 8129. (Bottom) 20°C isotherm (thermocline) depth (m), 1943–1988, n = 60,014. NET = north equatorial trough; CCR = countercurrent ridge; CCT = countercurrent trough; ER = equatorial ridge; and SET = south equatorial trough.

thermocline slopes upward toward the coasts of Peru and Baja California, reflecting the equatorward flow of the Peru and California Currents. These coastal systems feed into the eastern "upstream" ends of the NEC and SEC.

The westward, wind-driven transport of surface water in the tropical Pacific results in a downward slope of the sea surface of about half a meter from west to east. Westward wind stress exceeds the eastward pressure gradient force except in the doldrums, between the northeast and southeast trades. The North Equatorial Countercurrent (NECC) flows eastward between the NEC and SEC, on the southern flank of the countercurrent thermocline ridge. The NECC shows considerable seasonal variation, being strongest during November–December when the slope of the thermocline ridge is steepest (KESSLER and TAFT, 1987). These variations can be largely explained by local Ekman dynamics. The NECC lies in the Intertropical Convergence Zone (ITCZ) where the northeast and southeast tradewinds converge (the doldrums). Wind-stress curl is positive (cyclonic) over the countercurrent thermocline ridge at 10°N , causing Ekman upwelling. Wind-stress curl over the countercurrent thermocline trough at 5°N is negative (anticyclonic), causing Ekman downwelling. As the ITCZ migrates from its northern extreme in fall to its southern extreme in spring, the gradients in wind-stress curl and Ekman pumping velocity weaken, thermocline and sea surface slopes flatten, and flow of the NECC diminishes (FIEDLER, 1991). The phase and amplitude of the variations in the curl are sufficient to account for the variations in the depth of the thermocline ridge and the strength of the NECC (MEYERS, 1979; KESSLER and TAFT, 1987).

Upwelling occurs wherever horizontal divergence of surface waters causes subsurface water to ascend to conserve mass. Both coastal upwelling along eastern boundaries and equatorial upwelling occur in the ETP. Equatorial upwelling is the result of a geostrophic divergence of the wind-driven SEC. The westward component of the southeast trade winds causes poleward Ekman transport of surface water on either side of the equator. The effects of upwelling are evident in the equatorial thermocline ridge and in the anomalously cool temperature of equatorial surface water. SVERDRUP *et al.* (1942) presented evidence of surface divergence and upwelling at two sites in the equatorial current system: along the equator and between the NECC and NEC at 10°N. The countercurrent thermocline ridge is evidence of upwelling, although generally warm temperatures and low nutrient concentrations suggest that the effects of upwelling do not reach the surface (CROMWELL, 1953). Offshore transport of surface waters and coastal upwelling are driven by equatorward longshore winds along the coasts of Baja California and Peru, and by topographically-induced offshore winds at several points along the coast of Central America (Gulfs of Tehuantepec, Papagayo and Panama).

Equatorial water and coastal water (especially in the Peru Current System off Ecuador and Peru) in the ETP normally have a very high biological productivity (CHAVEZ and BARBER, 1987; BARBER and KOGELSCHATZ, 1990). Physical studies on both the coastal and equatorial regimes have shown that upwelled water is entrained usually from 40 to 80 m depth and always less than 100 m (SMITH, 1982; HALPERN and FREITAG, 1987). The thermocline is shallow in these regions, so that vertical advection and mixing bring cold, nutrient-rich water from below the thermocline (nutricline) into the surface layer. This nutrient input maintains optimal (saturating) concentrations of new nitrogen at the surface and results in high levels of new production (CHAVEZ and BARBER, 1987). Depression of the thermocline, as during El Niño, reduces the input of new nitrogen into the surface layer and limits productivity.

Interannual variability in the tropical Pacific Ocean is dominated by the El Niño–Southern Oscillation (ENSO). ENSO is an irregular cycle of variations in atmospheric pressure gradients, surface winds, sea surface temperature, thermocline depth, and biological productivity (CANE, 1983; GRAHAM and WHITE, 1988; ENFIELD, 1989). The response of the ETP to interannual wind variations caused by the Southern Oscillation (surface pressure difference between the Indonesian low pressure center at Darwin, Australia and South Pacific high pressure center at Tahiti) is similar to the response to seasonal variations, although the magnitude of the interannual response is much greater (PHILANDER, 1989). RASMUSSON and CARPENTER (1982) formulated a composite ENSO event from six events between 1949 and 1976. Relevant characteristics of each phase of the composite ENSO are listed in Table 1.

The interannual variability associated with the ENSO phenomenon since 1975 is shown by the variation of three indices: the Southern Oscillation Index (SOI), based on the sea-level pressure difference between Darwin and Tahiti; the NINO-3 (eastern equatorial Pacific) SST Anomaly; and the Southeast Trade Wind Anomaly (Fig. 3). The variability of these indices during 1986–1989 was extreme, ranging as widely as during the great 1982–1983 ENSO event. By these indices, the 1987 El Niño was beginning in mid-1986, when the Indonesian low was weakening (SOI decreasing) and SST in the eastern equatorial Pacific was becoming anomalously warm. At the same time, an operational model analysis of the tropical Pacific showed that the thermocline was deepening along the equator east of

Table 1. *Tropical Pacific surface temperature, pressure and trade winds in the Rasmusson–Carpenter composite El Niño–Southern Oscillation event* (*RASMUSSON and CARPENTER*, 1982)

Antecedent Phase
(a) Negative SST anomalies along Peru–Ecuador coast.
(b) South Pacific high pressure center weakening.
(c) Strong trade winds in the western Pacific.

Onset Phase (September of pre-El Niño year)
(a) SST near normal and rising along Peru–Ecuador coast. Positive SST anomalies in the central Pacific.
(b) South Pacific high reaches a minimum.
(c) Weak trade winds in the western and south Pacific.

Peak Phase (April of El Niño year)
(a) Positive SST anomalies in the eastern and central Pacific are spreading laterally and merging.
(b) Indonesian low approaching a maximum and Southern Oscillation Index approaching a maximum negative anomaly.
(c) Weak or reversed trade winds in the central Pacific.

Transition Phase (September of El Niño year)
(a) Large positive SST anomalies cover entire eastern and central equatorial Pacific, but are decreasing at Peru–Ecuador coast.
(b) South Pacific high is strengthening and SOI becoming less negative.
(c) Weak or reversed trade winds in central and western Pacific.

Mature Phase (January of post-El Niño year)
(a) Positive SST anomalies persist in eastern and central equatorial Pacific. Peru–Ecuador SSTs near normal.
(b) South Pacific high is normal and Indonesian low returning to normal.
(c) Strong trade winds in eastern equatorial Pacific.

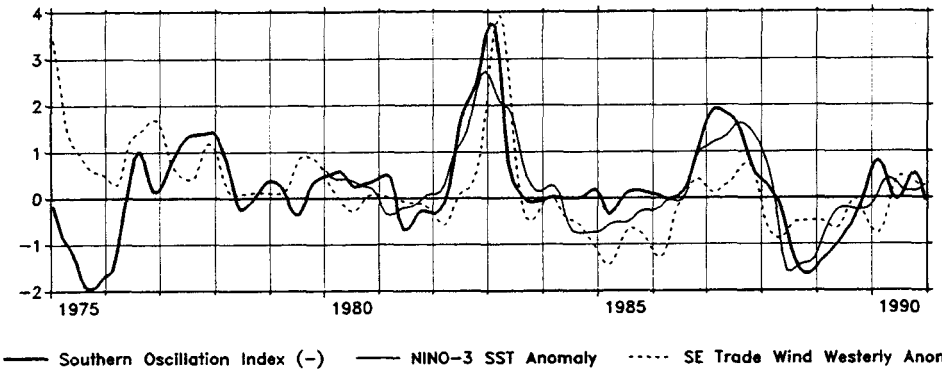

Fig. 3. Smoothed (4253H) monthly time series of (1) Southern Oscillation Index (−), the difference between standardized sea level pressure anomalies at Darwin and Tahiti (Darwin–Tahiti), (2) NINO-3 SST Anomaly, the mean sea surface temperature anomaly (°C) in the area 5°N–5°S and 150°W–90°W, and (3) Southeast Trade Wind Westerly Anomaly, the standardized 850 mb westerly wind anomaly in the area 5°N–5°S and 135°W–120°W. Note that the conventional signs of indices (1) and (3) are reversed, so that positive values of all indices indicate El Niño conditions. Monthly means from Climate Diagnostic Bulletin, NOAA/NWS/NMC/Climate Analysis Center.

150°W (KOUSKY and LEETMAA, 1989). The El Niño "peaked" during the fall of 1987. By late 1987 and early 1988 the indices had rapidly reversed sign and oceanic conditions were shifting to a cold phase, sometimes referred to as La Niña (PHILANDER, 1985). LANDER (1989) concluded that the 1986–1987 ENSO event was 3 months ahead of the Rasmusson–Carpenter composite, although this phase shift was within the range of variability of the six events included in the composite. MCPHADEN and HAYES (1990) pointed out that the 1986–1987 ENSO differed from the composite in that warm SST anomalies developed west of 140°W prior to South American coastal warming and that these warm anomalies persisted for 18 months, compared to 12 months in the composite.

Although ENSO events are not all alike, the composite ENSO of RASMUSSON and CARPENTER (1982) will be a useful point of reference in the discussion that follows. The seasonal cycle of variations in the ETP already discussed above will be second point of reference. Our observations are unique in the repeated intensive spatial coverage of a large oceanic region during a period of major environmental variability.

MATERIALS AND METHODS

NOAA Ships *McArthur* and *David Starr Jordan* surveyed a 14 million km^2 area each year from August to November, 1986–1989. Surface temperature, salinity and *in vivo* fluorescence data are collected continuously while the ships are underway (FIEDLER *et al.*, 1990). Four to six XBTs are deployed daily. CTD data and chlorophyll and nutrient samples are collected at one or two hydrographic stations per day (Table 2). We report here the XBT and hydrographic sample results.

In 1986, Niskin bottles were tripped at 20, 40, 60, 80, 100, 120, 140, 160, 180, 200, 500 and 1000 m. In 1987–1989, bottles were tripped at 20, 40, 60, 80, 100, 125, 150, 250, 350, 500 and 1000 m. Surface water samples were collected from the ships' seawater systems.

Table 2. Numbers of XBT and CTD casts completed, and nutrient and chlorophyll samples processed for this study

Year	XBT	CTD	Chlorophyll	Nutrient
1986	1678	344	4236	2010
1987	1176	280	2128	1577
1988	821	352	3613	1643
1989	743	352	3552	—
Total	4418	1328	13,529	5230

Chlorophyll and phaeopigments (down to 160 m) were determined by the fluorometric technique using Turner 111 fluorometers calibrated before and/or after each cruise with commercial chlorophyll *a* (Sigma*). Samples (275 ml) were filtered onto 25 mm Whatman GF/F or Gelman A/E glass-fiber filters and extracted for 24–36 h. A saturated magnesium carbonate solution filtered through the Gelman filters before filtering the sample improved retention of small cells (CHAVEZ and BARBER, 1987). Euphotic zone depth was calculated from total pigment profiles according to MOREL (1988).

Water samples for nutrient analysis (down to 500 m) were frozen immediately and returned to Duke University (1986) or Monterey Bay Aquarium Research Institute (MBARI, 1987–1988). Nitrate, nitrite, phosphate and silicate concentrations were determined on a Technicon (Duke) or Alpkem (MBARI) autoanalyzer. Nutrient samples from 1989 have not yet been analysed.

Data were objectively gridded in a 1° latitude–longitude grid using $1/d^2$ weighting ($0.1 \leq d \leq 4$ degrees). Grids were lightly smoothed before contouring (Laplacian smoothing, YOUNG and VAN WOERT, 1987). We statistically analysed the means of data in 2° squares to remove effects of spatial bias of the sampling design, which puts more effort in areas of greater dolphin abundance, and of changes in the distribution of effort between surveys. Interannual changes of chlorophyll and nutrient concentrations were determined by calculating ratios or differences of the 2° means. Contoured interannual ratio or difference maps were used to assess the spatial variability of interannual changes, but are not presented here.

RESULTS

Surface temperature and thermocline depth

In August–November 1986, we observed near-normal surface temperatures (anomalies of 0 to +1°C) and thermocline depths (anomalies of 0 to +20 m) over most of the ETP (Figs 4 and 5). However, along the equator west of 100°W and off the coast of Peru, the thermocline was depressed by 20–30 m and surface temperatures were >1°C above normal. SST anomalies also exceeded +1°C near the Galapagos. In tropical surface water north of the equator, surface temperatures were within about 0.5°C of normal and the depth of the countercurrent thermocline ridge was within 10 m of normal.

In August–November 1987, SST anomalies were +1°C or greater throughout most of the study area south of 10°N and were as large as +2 to +3°C along the equator (Fig. 4).

*Reference to trade name does not imply endorsement by NMFS.

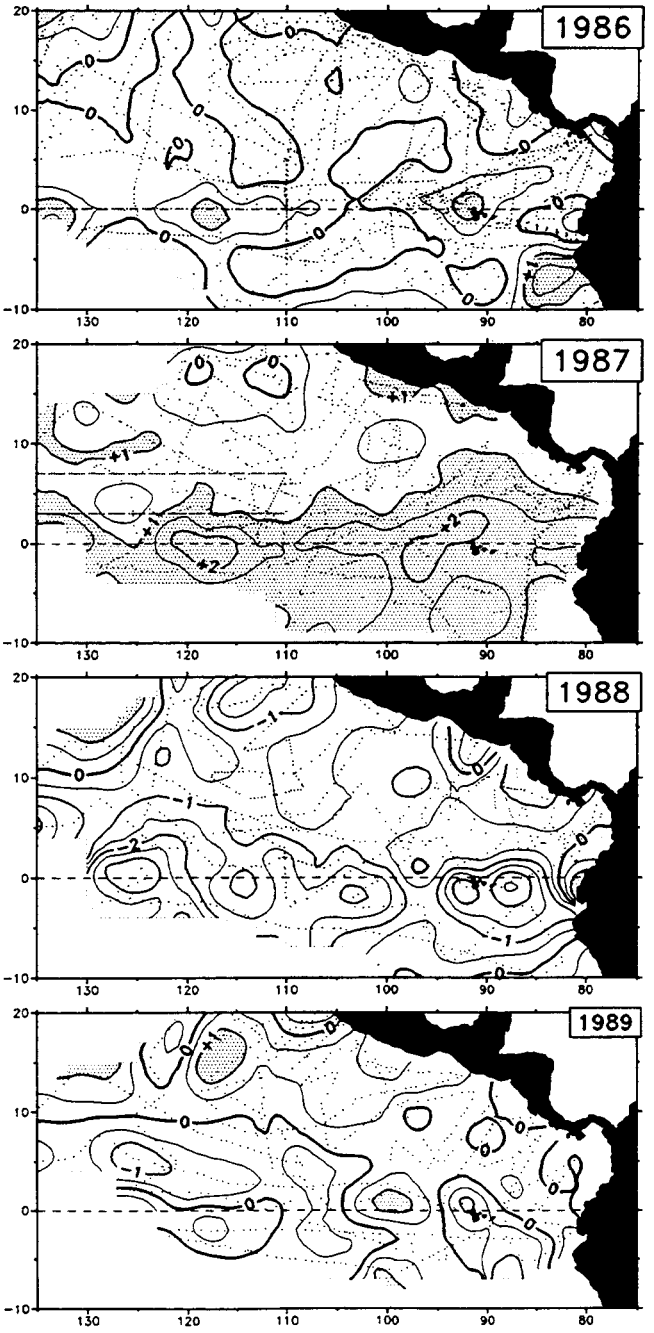

Fig. 4. Surface temperature anomalies (°C) from XBTs deployed on MOPS and EPOCS cruises, and by ships of opportunity, August–November 1986, 1987, 1988 and 1989.

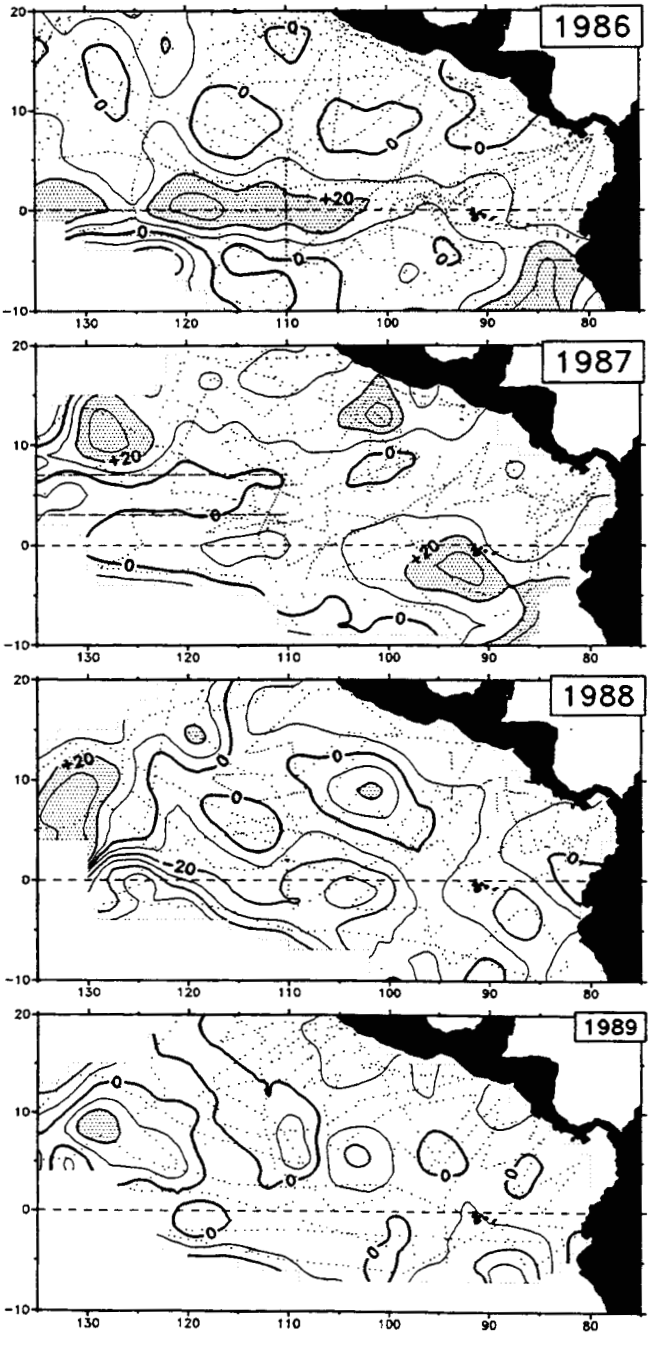

Fig. 5. Thermocline (20°C isotherm) depth anomalies (m) from XBTs, August–November 1986, 1987, 1988 and 1989.

The coldest SSTs in the equatorial cold tongue were only about 23°C, compared to normal SSTs of 21°C or less. The warm band of tropical surface water was warmer than 28°C across the entire study area (not shown). Thermocline depth anomalies appeared in tropical water north of the equator and thermocline topography was generally flatter than normal (Fig. 5). The basin-wide zonal slope was reduced by deepening in the extreme eastern tropical Pacific. Oceanic ridges and troughs were deepened and shoaled, respectively. Thermocline depth on the equator west of 110°W was closer to normal in 1987 than in 1986, although the equatorial thermocline ridge was depressed by 30 m south of the Galapagos.

By August–November 1988, surface temperatures were below normal over almost all of the study area (Fig. 4). The equatorial cold tongue was 0.5–2.5°C colder than normal and 2–4°C colder than in 1987. The 20°C isotherm had broken the surface as far west at 90°W, south of the Galapagos Islands; the coldest SSTs were less than 19°C (not shown). The warm, band of tropical surface water north of the equator had cooled by 1–2°C since 1987, but was not more than 1°C below normal. The equatorial thermocline ridge had shoaled to a depth of 20–40 m less than normal especially west of 100°W. The countercurrent ridge and trough were again well-developed, although the thermocline ridge remained anomalously deep west of 135°W and at the 100–110°W saddle (low point in the ridge, Fig. 2). The deep anomalies in the northwest corner of the study area and shallow (−10 m) anomalies along the Central American coast resulted in an unusually steep zonal thermocline slope.

In August–November 1989, we observed SST anomalies between −0.5 and +1.0°C and thermocline depths within ±10 m of normal over most of the study area. This year (1989) was the most normal (average) year in our 4-year time series.

Nutrients and chlorophyll

Although El Niño was beginning to affect surface temperature and thermocline structure in the central equatorial Pacific during August–November 1986, we will consider our nutrient and chlorophyll results from both 1986 and 1989 to represent "normal" conditions in the ETP. We present maps of nitrate concentration only (Figs 6 and 7), because phosphate and silicate were strongly correlated with nitrate (Table 3). In addition, regressions of phosphate and silicate on nitrate gave significant positive intercepts (all $P < 0.001$). This means that nitrate was depleted before phosphate or silicate and was more likely to limit productivity. Nitrate concentrations of <4 μg-at l^{-1} will be considered growth-limiting. At higher concentrations, nitrate uptake by oceanic phytoplankton is saturated (BARBER and KOGELSCHATZ, 1990).

In August–November 1986, surface nitrate concentrations were highest in equatorial water (south of 4°N) and in the region of the Costa Rica Dome (10°N, 90°W, Fig. 6).

Table 3. Regression analysis of phosphate (P) *and silicate* (S) *on nitrate* (N) *surface and mean euphotic zone concentrations* (μg-at l^{-1})

Phosphate		
Surface:	P = 0.06N + 0.32	$r = 0.82$
Euphotic zone:	P = 0.06N + 0.29	$r = 0.94$
Silicate		
Surface:	S = 0.39N + 1.84	$r = 0.77$
Euphotic zone:	S = 0.50N + 1.80	$r = 0.88$

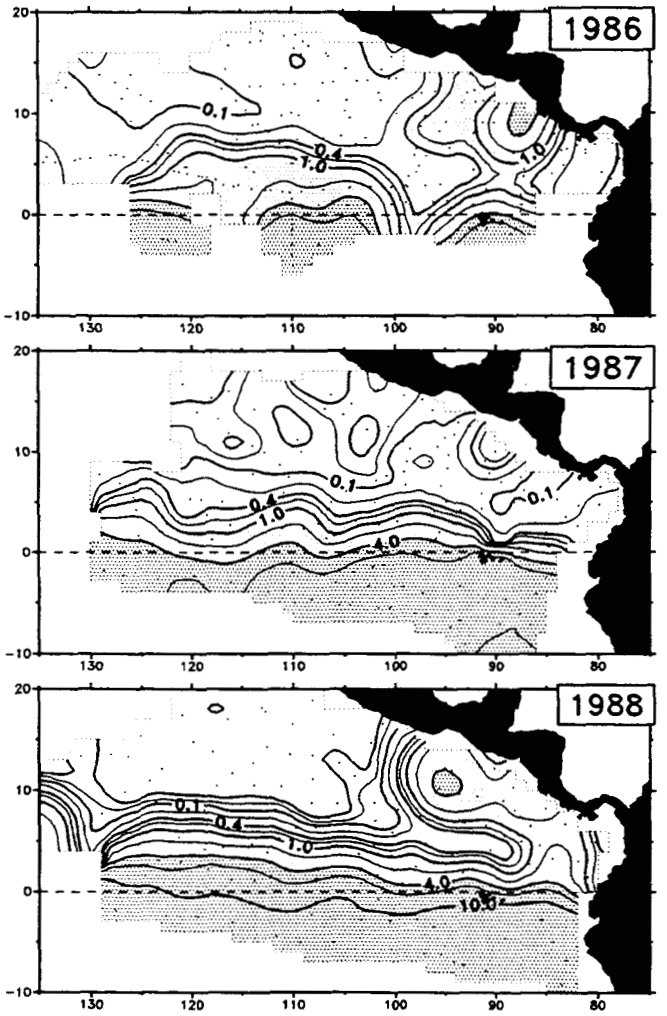

Fig. 6. Surface nitrate concentration (μg-at l^{-1}), August–November 1986, 1987 and 1988.

Nutrients supplied by equatorial upwelling sustained high chlorophyll standing stocks in a shallow euphotic zone south of 5°N, with concentrations increasing toward the coast of Ecuador and Peru (Figs 8 and 9). A band of high chlorophyll values extended approximately south of the Gulf of Tehuantepec in southern Mexico (16°N, 94°W), west of the elevated surface nutrients over the Costa Rica Dome. Euphotic zone nitrate concentrations were also high along 10°N. The lowest nitrate concentrations in this band occurred at the thermocline ridge saddle observed at 110–115°W. Chlorophyll concentrations were low in tropical water away from the influence of upwelling, decreasing to the west towards the oligotrophic North Pacific subtropical gyre.

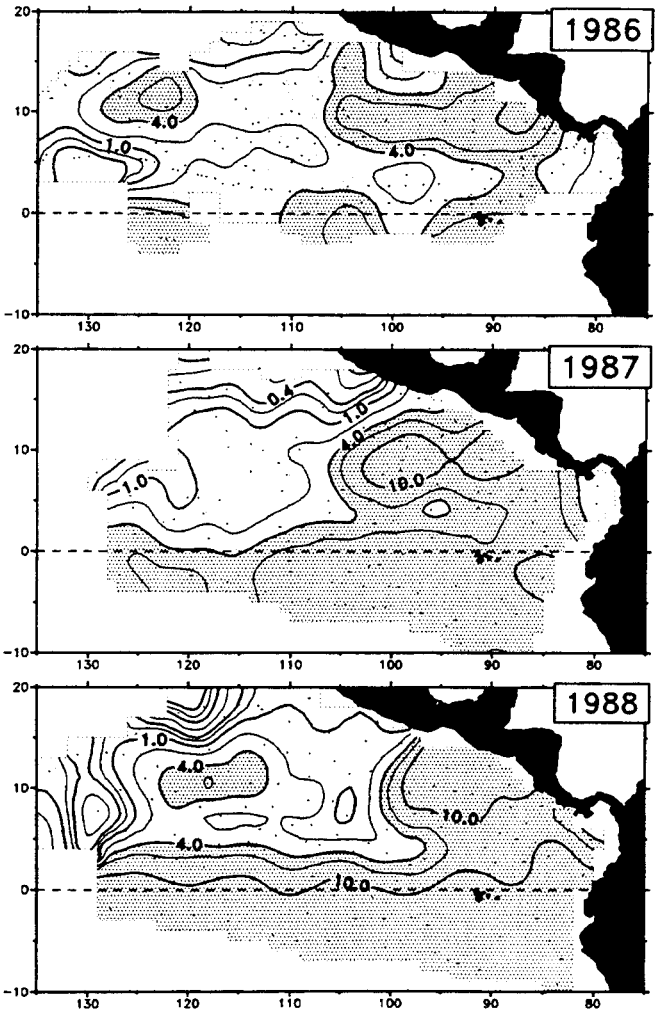

Fig. 7. Mean nitrate concentration (μg-at l^{-1}) in the euphotic zone, August–November 1986, 1987 and 1988.

In August–November 1987, surface nitrate concentrations were lower than in 1986 (Table 4). The greatest observed reductions in surface nutrients occurred in tropical water east of 105°W, where surface nitrate concentrations were less than half those observed in 1986. Overall, euphotic zone nitrate concentration did not change significantly between 1986 and 1987. However, the euphotic zone nitrate maximum band along the counter-current thermocline ridge extended only out to about 105°W in 1987 (Fig. 7). Concentrations in this band east of 105°W were higher than at the equator.

Chlorophyll concentrations were lower and the euphotic zone was deeper in 1987 than in 1986 (Table 5). The reduction in chlorophyll was greatest in equatorial water, especially

Table 4. Surface and mean euphotic zone nitrate concentrations (μg-at l^{-1}) and interannual ratios for the eastern tropical Pacific study area, August–November (medians of 2° square gridded means). The 1986 medians are biased by undersampling of equatorial water

Year	Surface	Euphotic zone
1986	(0.19)	(2.51)
1987	0.26	5.54
1988	1.13	5.80
1987/1986	0.52***	1.13
1988/1987	1.63***	1.60***
1988/1986	0.48***	1.35

Interannual differences tested by Wilcoxon signed ranks test: *, $P < 0.05$; **, $P < 0.01$; ***, $P < 0.001$.

west of 105°W, and in tropical water between 5 and 10°N west of 90°W, along the countercurrent thermocline ridge.

In August–November 1988, surface and mean euphotic zone nitrate concentrations were higher than in 1987 (Table 4). The greatest surface nitrate increases occurred in Central American coastal waters and in equatorial water west of 100°W. Surface nitrate concentrations, within the area north of the equator sampled in 1986, were surprisingly lower in 1988. Chlorophyll concentrations were higher and the euphotic zone was more shallow in 1988 than in 1987 (Table 5). The greatest surface chlorophyll increases occurred in the upwelling systems along the equator near the Galapagos and in coastal waters near

Table 5. Median surface chlorophyll concentrations (mg m^{-3}) and interannual ratios, and mean euphotic zone depths (m) and interannual differences for the eastern tropical Pacific study area, August–November

Year	Surface chlorophyll	Euphotic zone	
		Chlorophyll	Depth
1986	0.18	0.23	60.2
1987	0.13	0.19	69.2
1988	0.21	0.28	54.4
1989	0.19	0.25	58.0
1987/1986	0.77***	0.85***	+8.6***
1988/1987	1.65***	1.58***	−15.4***
1989/1988	0.89***	0.90***	+4.1***
1989/1986	1.14***	1.10***	−2.2***

Interannual differences tested by Wilcoxon signed ranks test (chlorophyll) or paired *t*-test (euphotic zone depth): *, $P < 0.05$; **, $P < 0.01$; ***, $P < 0.001$.

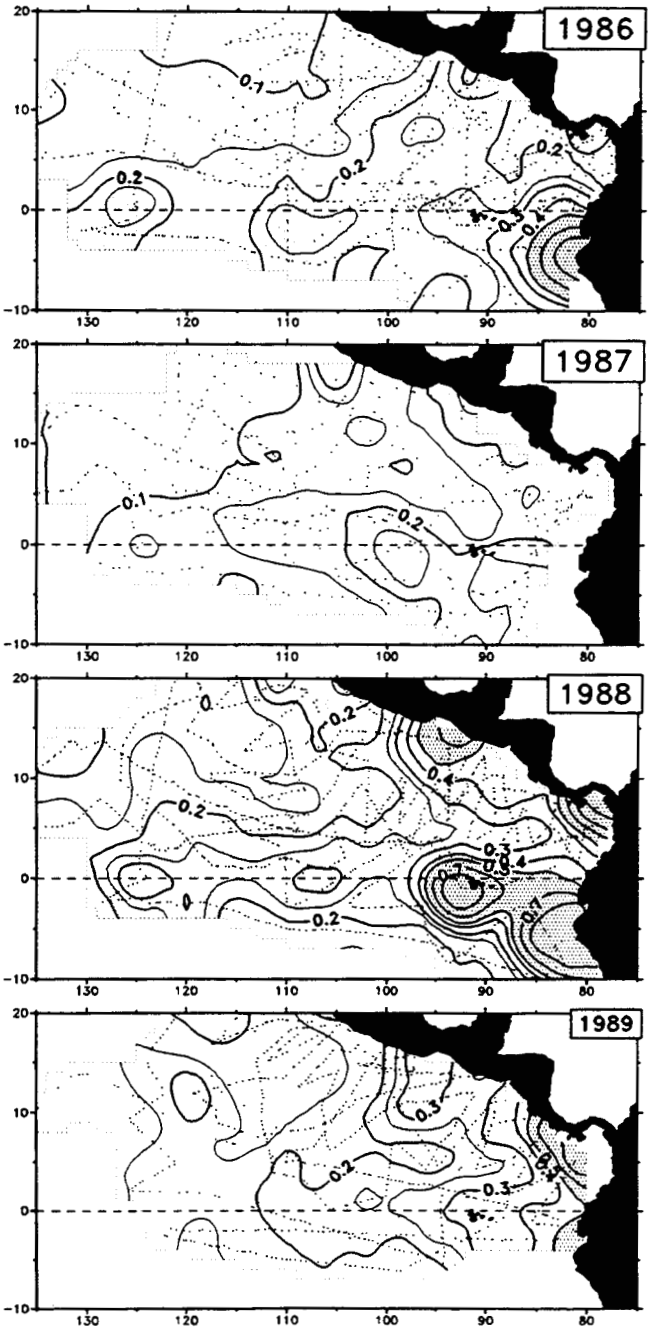

Fig. 8. Surface chlorophyll concentration (mg m^{-3}), August–November 1986, 1987, 1988 and 1989.

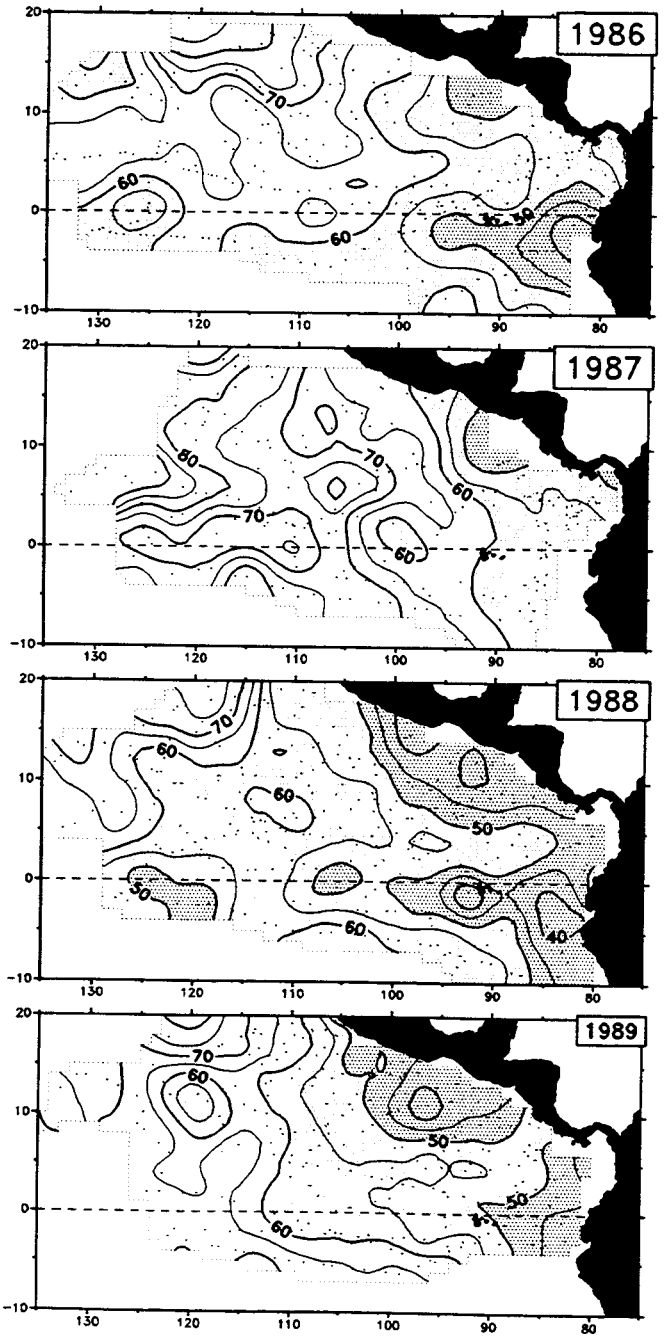

Fig. 9. Euphotic zone depth (m), calculated from phytoplankton pigment profiles (MOREL, 1988), August–November 1986, 1987, 1988 and 1989.

the Gulf of Tehuantepec and in the Gulf of Panama. Increases in subsurface chlorophyll, indicated by a decreasing euphotic zone depth, were greatest to the west of 110°W, where euphotic zone nitrate increased.

In August–November 1989, chlorophyll concentrations were lower and the euphotic zone was deeper than in 1988 (Table 5). The greatest changes occurred in equatorial water and along the coast of Central America north of 10°N. Compared to 1986, chlorophyll concentrations overall were still slightly elevated and the euphotic zone was shoaled by 2 m in 1989.

DISCUSSION

Physical effects

We observed the beginning of an El Niño event in the ETP in August–November 1986: anomalously warm surface temperatures and a depressed thermocline in equatorial water west of 100°W and off the coast of Peru. In terms of the composite ENSO (RASMUSSON and CARPENTER, 1982), these months would include the "Antecedent Phase" and just precede the "Onset Phase" of an ENSO event reaching its full development in 1987. The composite SST anomaly field shows positive values confined south of 10°S in the ETP for this phase. Only during the "Peak Phase" in the following spring does the composite SST anomaly field show positive values along the equator. In terms of the annual cycle of the SST field, warming along the equator should occur during the spring, beginning in the east and propagating westward. At this stage, the 1986–1987 event appears to be leading the composite event by 3 months (LANDER, 1989; KOUSKY and LEETMAA, 1989). Also, the warming of the surface waters in the ETP does not appear to be a simple enhancement of the annual cycle.

By late 1987, the Southern Oscillation Index had begun to return to normal and the eastern equatorial Pacific SST anomaly had reached a maximum (Fig. 3). We observed anomalously warm surface temperatures throughout the study area, with the warmest anomalies in equatorial water. Thermocline topography was generally flatter than normal. The slope between the countercurrent thermocline trough and ridge (5–10°N) was reduced, suggesting a weakened North Equatorial Countercurrent. WYRKTI (1974) showed that the NECC was anomalously strong in the central Pacific during El Niño years, but we did not sample the "peak" phase of the event when the NECC may have been stronger. In the 1982–1983 El Niño, the NECC was anomalously strong in the early stages of the event, but anomalously weak after December 1982 (MEYERS and DONGUY, 1984; KESSLER and TAFT, 1987).

In terms of the composite ENSO (RASMUSSON and CARPENTER, 1982), the "Transition Phase" of the event would occur in the months of August–October 1987. For this period, in the ETP, the composite SST anomaly field shows positive values throughout the region south of 10°N, with equatorial values exceeding +1.5°C. Composite SST anomalies for the "Mature Phase" occurring a few months later show a similar pattern. Our 1987 observations are consistent with these patterns. In terms of the annual cycle, the months of August–November encompass the warmest time of the year for SSTs in the tropical surface water and the coolest time for SSTs in the cold equatorial tongue. Along with the weakened NECC, this would account for the warmer surface temperature anomalies in equatorial water.

The "Mature Phase" of the composite ENSO ends abruptly with a rapid decline of coastal SST anomalies early in the year following the event (RASMUSSON and CARPENTER, 1982). In the first 4 months of 1988, the eastern equatorial Pacific SST anomaly declined from more than +1 to less than −1°C (Fig. 3). We observed anomalously cool surface temperatures and a shallow thermocline over most of the study area, especially in equatorial water west of 100°W. This indicates strengthened SEC flow and equatorial upwelling. The unusually steep zonal thermocline slope north of the equator suggests a strengthened southward flow of cool California Current water into the ETP, which may have contributed to the negative SST anomalies in tropical water during La Niña 1988.

The 1986–1987 El Niño event was less intense than the 1982–1983 event in terms of anomalies in surface temperature, near-surface flow and winds (Fig. 3; MCPHADEN and HAYES, 1990). Both events began similarly, with warm SST anomalies developing in mid-year in the central Pacific, prior to the South American coastal warming (KOUSKY and LEETMAA, 1989). Both events were terminated in the ETP by wind events in the central and western Pacific. However, the 1986–1987 El Niño event lasted longer (18 months compared to 12 months in 1982–1983) and was followed by a more intense La Niña event.

The most nearly normal (average) year in this study was 1989 for ETP surface temperature and thermocline depth. By the end of the year, the surface layer of the western equatorial Pacific was anomalously warm and deep. Westerly trade wind anomalies and increased convective activity in the western and central Pacific suggested an incipient El Niño event (KOUSKY, 1990). However, the event had not developed in the ETP by the end of 1990.

Biological effects

Previous studies of the biological effects of ENSO variability, at the primary producer level, have relied on data from single equatorial or coastal transects or stations (DANDONNEAU and DONGUY, 1983; BARBER and CHAVEZ, 1983, 1986; KOGELSCHATZ *et al.*, 1985). Our data provide the first large-scale view of the biological effects of interannual ENSO variability in equatorial, tropical and coastal waters of the eastern tropical Pacific.

Surface nitrate concentrations in the ETP are highest in equatorial and coastal upwelling regions (Fig. 6). Warm tropical water, beyond the influence of upwelling, has very low nitrate concentrations at the surface. However, mean euphotic zone nitrate concentrations are relatively high in tropical water along 10°N, at the countercurrent thermocline ridge, where the euphotic zone extends below the thermocline (compare Figs 5 and 9). Euphotic zone nitrate concentrations at the countercurrent thermocline ridge are often equal to or greater than values at the equator (Fig. 7). Surface chlorophyll levels are not elevated above this ridge (Fig. 6). However, the euphotic zone deepens over the countercurrent thermocline trough north of the equator and then shoals at the ridge (Fig. 9), suggesting that nutrient input results in increased chlorophyll below the surface.

Upwelling of limiting nutrients from below a shallow thermocline results in high levels of new production in the eastern equatorial Pacific and in Peru coastal waters. Productivity of equatorial and coastal upwelling waters is reduced during El Niño because the thermocline is depressed below the depth of entrainment, so that the upwelled water is warm and depleted of nutrients (BARBER and CHAVEZ, 1986; BARBER and KOGELSCHATZ, 1990). In addition, upwelling-favorable winds (easterly trades) along the equator are reduced (Fig. 3). The greatest relative reductions in nutrient availability between 1986 and 1987 were

observed in tropical water north of the equator. However, the most critical change for phytoplankton productivity is represented by changes in the extent of nutrient-rich water (>4 μg-at l^{-1} nitrate). Equatorial waters remained nutrient-rich in 1987, although nutrient-rich conditions did not extend north of the equator.

We observed a reduction in chlorophyll standing stock that could have been caused by depression of the thermocline during El Niño, leading to reduced transport of nutrients to the surface and lower biological productivity. The equatorial and countercurrent thermocline ridges were anomalously deep in 1987 (Fig. 5), reducing nutrient input from below the thermocline. However, nitrate concentration in equatorial water did not become limiting in 1987, at least in our August–November observations. The equatorial thermocline ridge actually shoaled west of 105°W between fall 1986 and fall 1987. The only part of the study area where we observed a change from nutrient-rich to nutrient-poor conditions was in subsurface waters along the countercurrent thermocline ridge west of 105°W (Fig. 7). BARBER and CHAVEZ (1983, 1986) observed nutrient-depleted water along the equator and 5°S to the coast of Peru in April and May 1983. Normal, nutrient-rich conditions had returned by the next observations in November and July, respectively. Thus, we may have missed a more pronounced thermocline depression and nitrate reduction in equatorial water earlier in 1987.

The countercurrent thermocline ridge normally lies as close to the surface as the equatorial ridge to the south at the same longitude, except at the 100–110°W saddle (Fig. 2). Euphotic zone nutrient concentrations above this ridge are as high as at the equator, although nutrients are depleted at the surface (Figs 6 and 7). We observed chlorophyll reductions in this region as great as at the equator (by as much as 50% between 1986 and 1987). These reductions can be explained by observed thermocline depression and lower nutrient availability. However, the pelagic ecosystem over this ridge is functionally different than the equatorial ecosystem: surface nutrient concentrations and chlorophyll standing stock are very low (surface waters more oligotrophic than eutrophic), although enhanced zooplankton standing stocks comparable to those at the equator have been observed (BRANDHORST, 1985; REID, 1962).

We observed major changes in nutrient availability between El Niño 1987 and La Niña 1988. The thermocline shoaled by 20 m or more along both the equator and the Central American coast (Fig. 5), where the greatest surface nitrate increases occurred. Nutrient-rich (>4 μm nitrate) surface water extended up to 400 km north of the equator (Fig. 6). Surface and euphotic zone nitrate concentrations exceeded 10 μg-at l^{-1} in equatorial water. Chlorophyll concentrations increased greatly, especially in the upwelling systems along the equator and in Central American coastal waters.

These results are consistent with increased productivity caused by increased upwelling of nutrient-rich water from below the shoaled thermocline/nutricline during La Niña. If El Niño and La Niña are complementary extremes in a cycle of variable biological productivity in the ETP, then the 1988/1987 change lends additional support to the hypothesis that reduced chlorophyll concentrations in 1987 were the result of productivity limited by anomalously low nutrient input in coastal and equatorial upwelling regions.

Acknowledgements—Many people helped collect these data. We thank Victoria Thayer (formerly SWFSC), Julie Ellison (PMC), Gregg Thomas (AOML), and Lisa Lierheimer, Robert Holland and Robert Owen (SWFSC), as well as the officers and crew of the *David Starr Jordan* and *McArthur*. Thea Brower (Duke University) and Carol Sakamoto (MBARI) performed the nutrient analyses. Maps were drawn using PLOT88.

REFERENCES

BARBER R. T. and F. P. CHAVEZ (1983) Biological consequences of El Niño. *Science*, **222**, 1203–1210.

BARBER R. T. and F. P. CHAVEZ (1986) Ocean variability in relation to living resources during the 1982–83 El Niño. *Nature*, **319**, 279–285.

BARBER R. T. and J. E. KOGELSCHATZ (1990) Nutrients and productivity during the 1982/83 El Niño. In: *Global ecological consequences of the 1982–83 El Niño–Southern Oscillation*, P. W. GLYNN, editor, Elsevier, Amsterdam, pp. 21–53.

BLACKBURN M., R. M. LAURS, R. W. OWEN and B. ZEITZSCHEL (1970) Seasonal and areal changes in standing stocks of phytoplankton, zooplankton and micronekton in the eastern tropical Pacific. *Marine Biology*, **7**, 14–31.

BRANDHORST W. (1958) Thermocline topography, zooplankton standing crop, and mechanisms of fertilization in the eastern tropical Pacific. *Journal Conseil International pour Exploration de la Mer*, **24**, 16–31.

BRYDEN H. L. and E. C. BRADY (1985) Diagnostic model of the three-dimensional circulation in the upper equatorial Pacific Ocean. *Journal of Physical Oceanography*, **15**, 1255–1273.

CANE M. A. (1983) Oceanographic events during El Niño. *Science*, **222**, 1189–1194.

CHAVEZ F. P. and R. T. BARBER (1987) An estimate of new production in the equatorial Pacific. *Deep-Sea Research*, **24**, 1229–1243.

CROMWELL T. (1953) Circulation in a meridional plane in the central equatorial Pacific. *Journal of Marine Research*, **12**, 196–213.

DANDONNEAU Y. and J.-R. DONGUY (1983) Changes in sea surface chlorophyll concentration related to the 1982 El Niño. *Tropical Ocean–Atmosphere Newsletter*, **21**, 14–15.

DONGUY J.-R. and G. MEYERS (1987) Observed and modelled topography of the 20°C isotherm in the tropical Pacific. *Oceanologica Acta*, **10**, 41–48.

ENFIELD D. B. (1989) El Niño, past and present. *Reviews of Geophysics*, **27**, 159–187.

FIEDLER P. C. (in press) Seasonal variability of eastern tropical Pacific surface waters. NOAA Technical Report NMFS.

FIEDLER P. C., S. B. REILLY, S. N. SEXTON, R. S. HOLT and D. P. DEMASTER (1990) Atlas of eastern tropical Pacific oceanographic variability and cetacean sightings, 1986–1988. NOAA Technical Memorandum NMFS-SWFSC **144**, 142 pp.

GRAHAM N. E. and W. B. WHITE (1988) The El Niño cycle: a natural oscillator of the Pacific ocean–atmosphere system. *Science*, **240**, 1293–1302.

HAYES S. P., D. W. BEHRINGER, M. BLACKMON, D. V. HANSEN, N.-C. LAU, A. LEETMAA, S. G. H. PHILANDER, E. J. PITCHER, C. S. RAMAGE, E. M. RASMUSSON, E. S. SARACHIK and B. A. TAFT (1986) The Equatorial Pacific Ocean Climate Studies (EPOCS) Plans: 1986–1988. *EOS*, **67**, 442–444.

HALPERN D. and P. FREITAG (1987) Vertical motion in the upper ocean of the equatorial eastern Pacific. *Oceanologica Acta*, Vol. Spec., No. **6**, 19–26.

HOREL J. D. (1982) On the annual cycle of the tropical Pacific atmosphere and ocean. *Monthly Weather Review*, **110**, 1863–1878.

KESSLER W. S. (1990) Observations of long Rossby waves in the northern tropical Pacific. *Journal of Geophysical Research*, **95**, 5183–5217.

KESSLER W. S. and B. A. TAFT (1987) Dynamic heights and zonal geostrophic transports in the central tropical Pacific during 1979–84. *Journal of Physical Oceanography*, **17**, 97–122.

KOGELSCHATZ J., L. SOLORZANO, R. BARBER and P. MENDOZA (1985) Oceanographic conditions in the Galapagos Islands during the 1982/83 El Niño. In: *El Niño in the Galapagos Islands: the 1982/1983 Event*, G. ROBINSON and E. M. DEL PINO, editors, Charles Darwin Foundation for the Galapagos Islands, Quito, Ecuador, pp. 91–123.

KOUSKY V. E., editor (1990) *Climate Diagnostics Bulletin*. NOAA/National Weather Service/Climate Analysis Center.

KOUSKY V. E. and A. LEETMAA (1989) The 1986–87 Pacific warm episode: evolution of oceanic and atmospheric anomaly fields. *Journal of Climate*, **2**, 254–267.

LANDER M. A. (1989) A comparative analysis of the 1987 ENSO event. *Tropical Ocean–Atmosphere Newsletter*, **49**, 3–6.

LEETMAA A. (1983) The role of local heating in producing temperature variations in the offshore waters of the eastern tropical Pacific. *Journal of Physical Oceanograqphy*, **13**, 467–473.

McCreary J. P., H. S. Lee and D. B. Enfield (1989) The response of the coastal ocean to strong offshore winds: with application to circulations in the Gulfs of Tehuantepec and Papagayo. *Journal of Marine Research*, **47**, 81–109.

McPhaden M. J. and S. P. Hayes (1990) Variability in the eastern equatorial Pacific Ocean during 1986–1988. *Journal of Geophysical Research*, **95**, 13,195–13,208.

Meyers G. (1979) On the annual Rossby wave in the tropical North Pacific Ocean. *Journal of Physical Oceanography*, **9**, 663–674.

Meyers G. and J.-R. Donguy (1984) The North Equatorial Countercurrent and heat storage in the western pacific Ocean during 1982–83. *Nature*, **312**, 258–260.

Morel A. (1988) Optical modeling of the upper ocean in relation to its biogenous matter content (Case I waters). *Journal of Geophysical Research*, **93**, 10,749–10,768.

Perrin W. F. (1969) Using porpoise to catch tuna. *World Fishing*, **18**, 42–45.

Philander S. G. H. (1985) El Niño and La Niña. *Journal of Atmospheric Science*, **42**, 2652–2662.

Philander S. G. H. (1989) *El Niño, La Niña, and the Southern Oscillation*. Academic Press, New York, 293 pp.

Rasmusson E. M. and T. H. Carpenter (1982) Variations in tropical sea surface temperature and surface wind fields associated with the Southern Oscillation/El Niño. *Monthly weather Review*, **110**, 354–384.

Reid J. L. (1962) On circulation, phosphate–phosphorus content, and zooplankton volumes in the upper part of the Pacific Ocean. *Limnology and Oceanography*, **7**, 287–306.

Smith R. L. (1982) Circulation patterns in upwelling regimes. In: *Coastal upwelling: its sediment record*, E. Suess and J. Thiede, editors, NATO Advanced Research Institute Proceedings, Plenum Press, New York, pp. 13–37.

Sverdrup H. U., M. W. Johnson and R. H. Fleming (1942) *The oceans: their physics, chemistry and general biology*, Prentice-Hall, Englewood Cliffs, New Jersey, 1087 pp.

Wyrtki K. (1966) Oceanography of the eastern equatorial Pacific Ocean. *Oceanography and Marine Biology Annual Review*, **4**, 33–68.

Wyrtki K. (1967) Circulation and water masses in the eastern equatorial Pacific Ocean. *International Journal of Oceanology and Limnology*, **1**, 117–147.

Wyrtki K. (1974) Equatorial currents in the Pacific 1950 to 1970 and their relations to the trade winds. *Journal of Physical Oceanography*, **4**, 372–380.

Wyrtki K. (1981) An estimate of equatorial upwelling in the Pacific. *Journal of Physical Oceanography*, **11**, 1205–1214.

Young T. L. and M. L. van Woert (1989) PLOT88 Software Library Reference Manual, 3rd edn, Plotworks, Ramona, California, 342 pp.